

Electronic Supplementary Information

Photoinduced energy and charge transfer in bis(triphenylamine)-BODIPY- C₆₀ artificial photosynthetic system

Jian-Yong Liu*, Xue-Ni Hou, Ye Tian, Lizhi Jiang, Shuiquan Deng,

Beate Röder and Eugeny A. Ermilov*

Contents

- Fig. S1** Fluorescence spectra of triad **4** (*a*) and tetrad **6** (*b*) in polar DMF and nonpolar TOL upon excitation at 613 nm (BODIPY-part excitation). Optical density of the samples was adjusted to 0.1 at the BODIPY absorption maximum.
- Fig. S2** Fit of the Δ OD signal at 550 nm of triad **4** solved in DMF (*a*) and TOL (*b*).
- Fig. S3** Fit of the Δ OD signal at 550 nm of tetrad **6** solved in DMF (*a*) and TOL (*b*).
- Fig. S4** Differential pulse voltammetry of tetrad **6** in deaerated DMF in the presence of 0.1 M [*n*-Bu₄N][ClO₄]. Scan rate = 20 mV s⁻¹.
- Table S1** Vertical transition wavelengths λ_{max} (nm), transition energies ΔE (eV) and transition contributions calculated at TD-DFT B3LYP/(cc-pVDZ) level.
- Fig. S5** Energy level diagram showing the different photophysical events of tetrad **6** in TOL.
- Fig. S6** ¹H NMR spectrum of **3**.
- Fig. S7** ¹³C {¹H} NMR spectrum of **3**.
- Fig. S8** HRMS spectrum of **3**.
- Fig. S9** ¹H NMR spectrum of **4**.
- Fig. S10** ¹³C {¹H} NMR spectrum of **4**.
- Fig. S11** HRMS spectrum of **4**.
- Fig. S12** ¹H NMR spectrum of **5**.

Fig. S13 $^{13}\text{C}\{^1\text{H}\}$ NMR spectrum of **5**.

Fig. S14 HRMS spectrum of **5**.

Fig. S15 ^1H NMR spectrum of **6**.

Fig. S16 HRMS spectrum of **6**.

Fig. S17 ^1H NMR spectrum of **9**.

Fig. S18 MS spectrum of **9**.

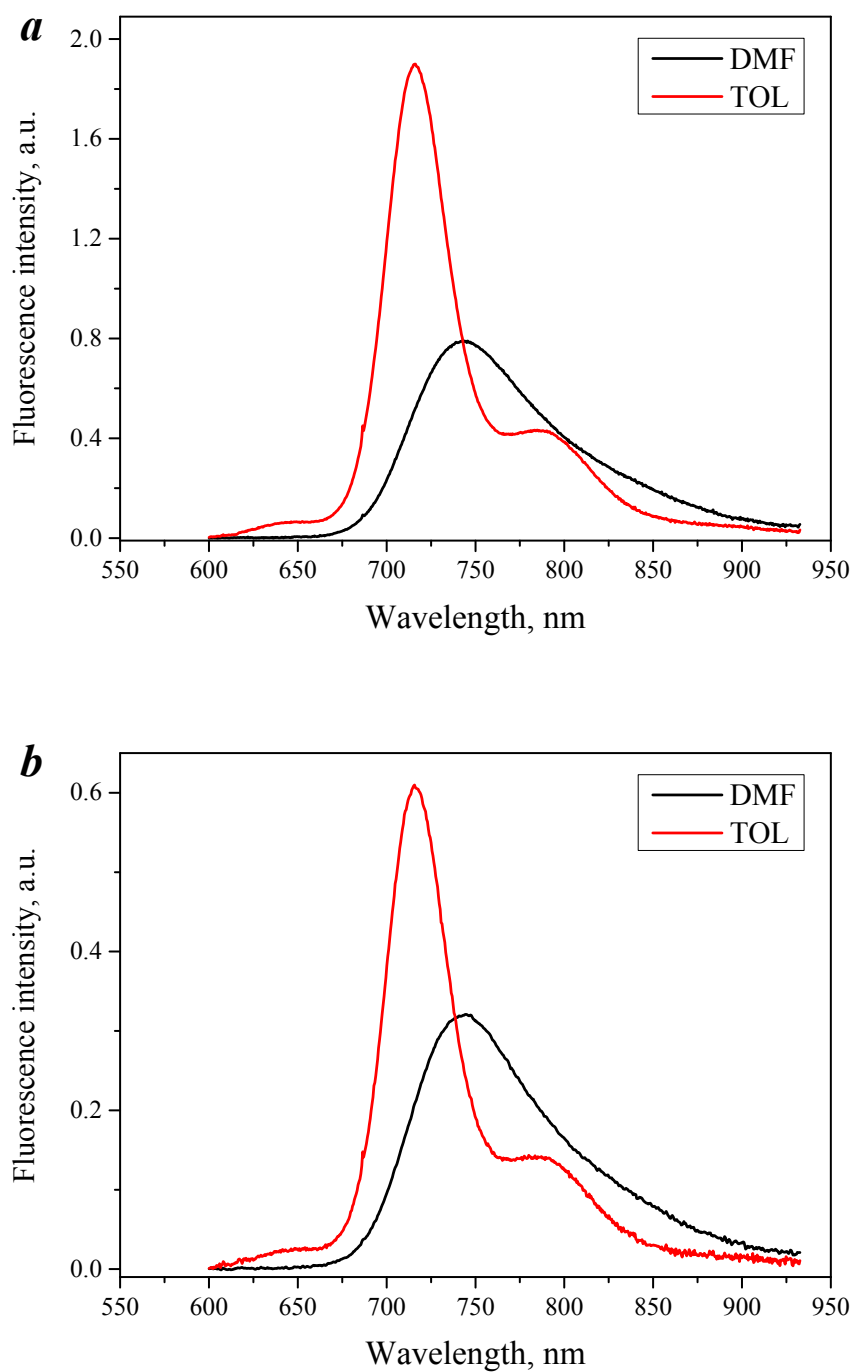


Fig. S1 Fluorescence spectra of triad **4** (*a*) and tetrad **6** (*b*) in polar DMF and nonpolar TOL upon excitation at 613 nm (BODIPY-part excitation). Optical density of the samples was adjusted to 0.1 at the BODIPY absorption maximum

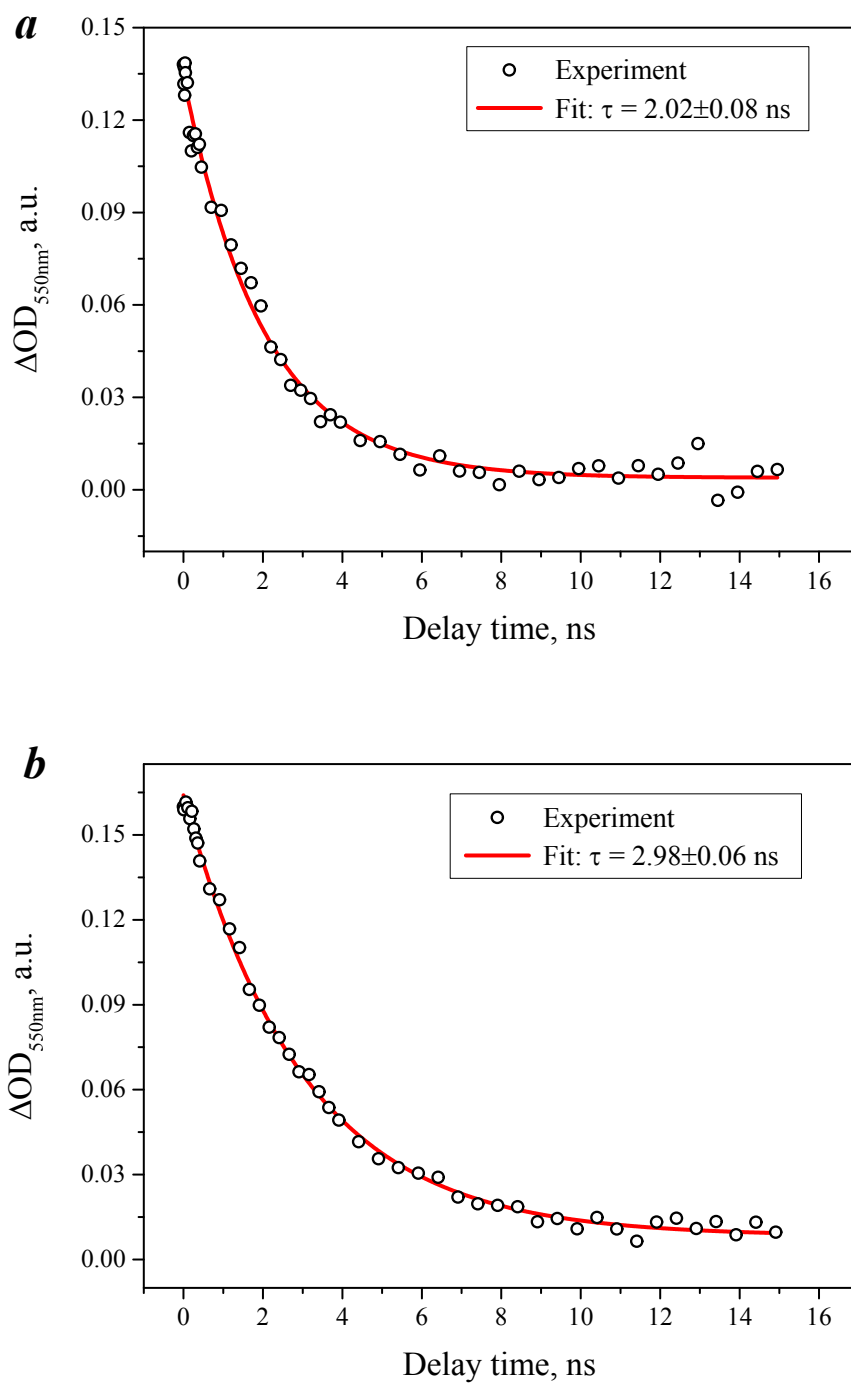


Fig. S2 Fit of the ΔOD signal at 550 nm of triad **4** solved in DMF (*a*) and TOL (*b*)

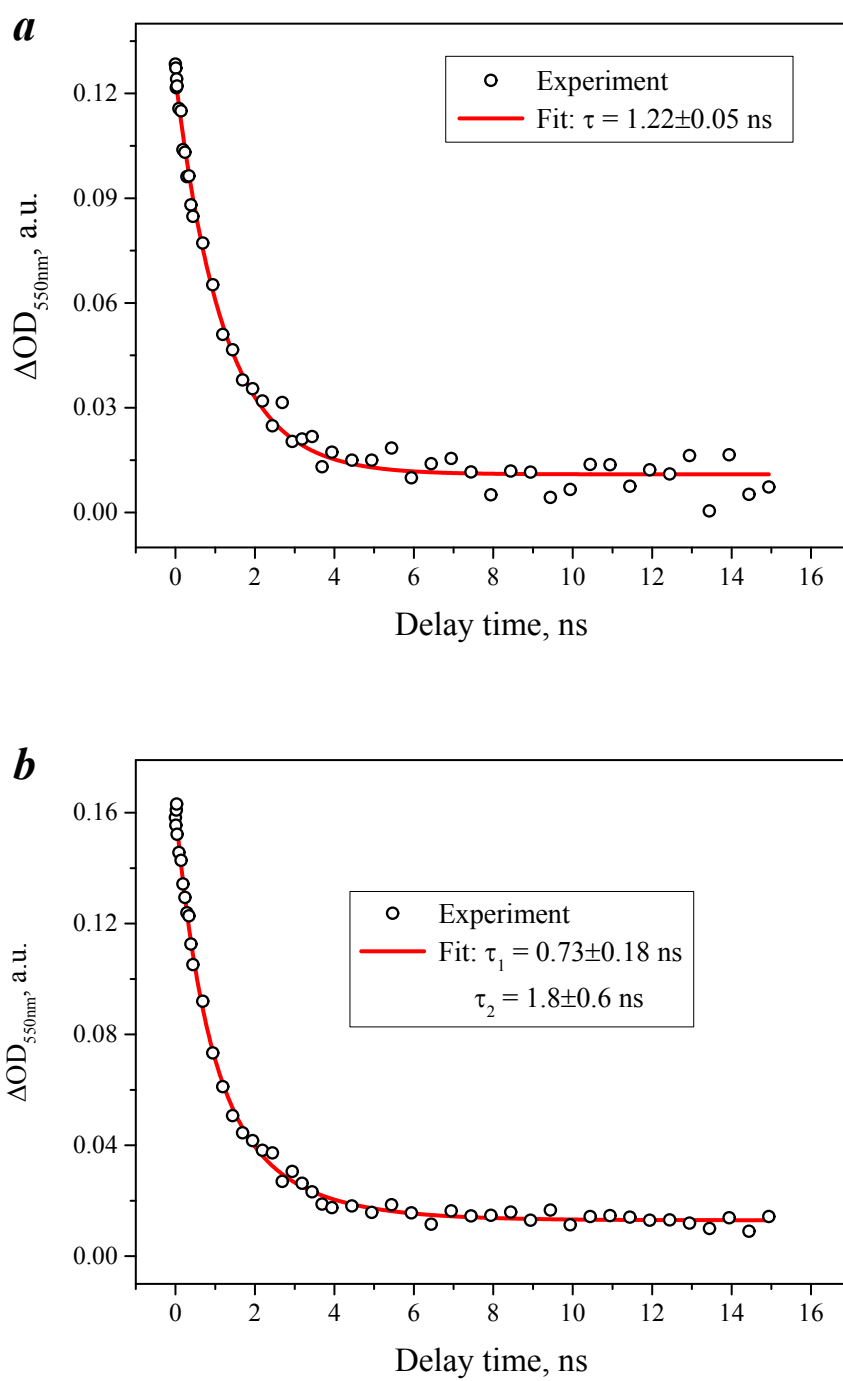


Fig. S3 Fit of the ΔOD signal at 550 nm of tetrad **6** solved in DMF (**a**) and TOL (**b**)

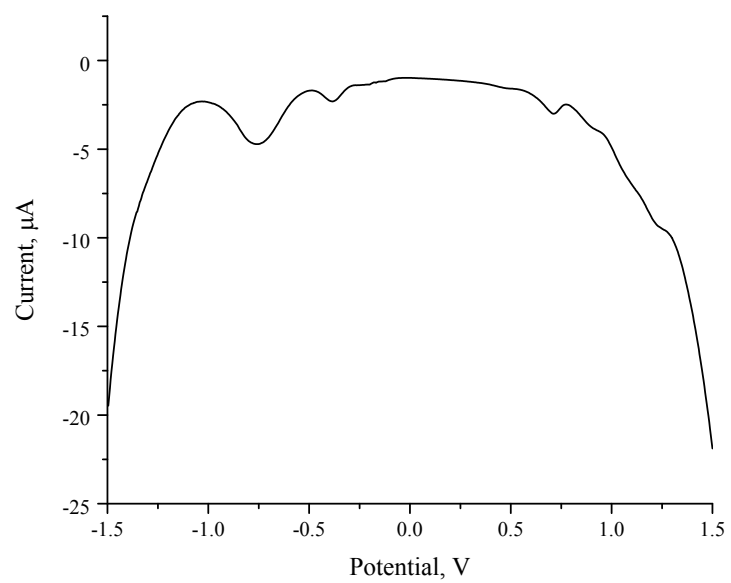


Fig. S4 Differential pulse voltammetry of tetrad **6** in deaerated DMF in the presence of 0.1 M $[n\text{-Bu}_4\text{N}][\text{ClO}_4]$. Scan rate = 20 mV s^{-1}

Table S1 Vertical transition wavelengths λ_{\max} (nm), transition energies ΔE (eV) and transition contributions calculated at TD-DFT B3LYP/(cc-pVDZ) level

Compound	λ_{\max} (nm)	ΔE (eV)	Transitions (contribution)
2	535	2.32	HOMO \rightarrow LUMO (100%)
	387	3.20	HOMO-3 \rightarrow LUMO (63%) HOMO-1 \rightarrow LUMO (36%)
4	708	1.75	HOMO \rightarrow LUMO (99%)
	561	2.21	HOMO-1 \rightarrow LUMO (96%)
	405	3.06	HOMO \rightarrow LUMO+1 (71%) HOMO-3 \rightarrow LUMO (25%)
	371	3.34	HOMO-3 \rightarrow LUMO (41%) HOMO-4 \rightarrow LUMO (17%) HOMO \rightarrow LUMO+1 (16%)
	353	3.51	HOMO \rightarrow LUMO+3 (38%)
6	712	1.74	HOMO \rightarrow LUMO+3 (92%)
	568	2.18	HOMO-1 \rightarrow LUMO+3 (95%)

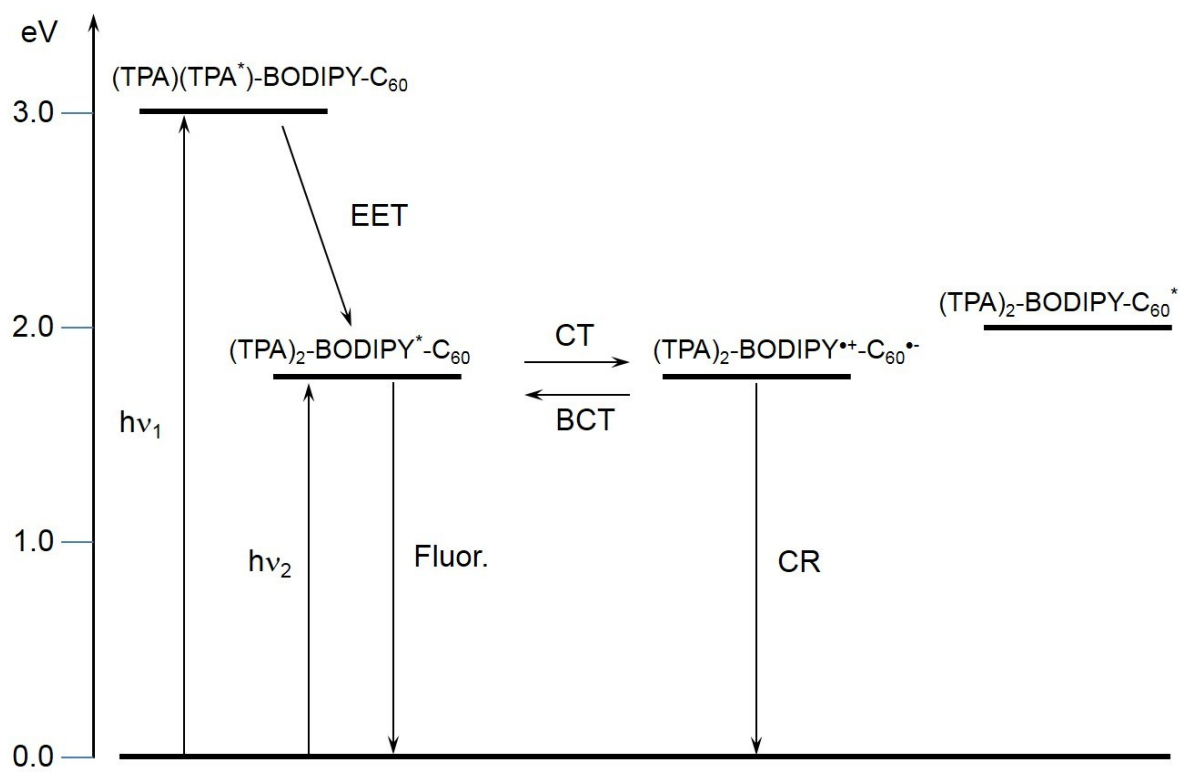


Fig. S5 Energy level diagram showing the different photophysical events of tetrad **6** in TOL

In all of the following spectra, the residual solvent signals are marked with asterisks

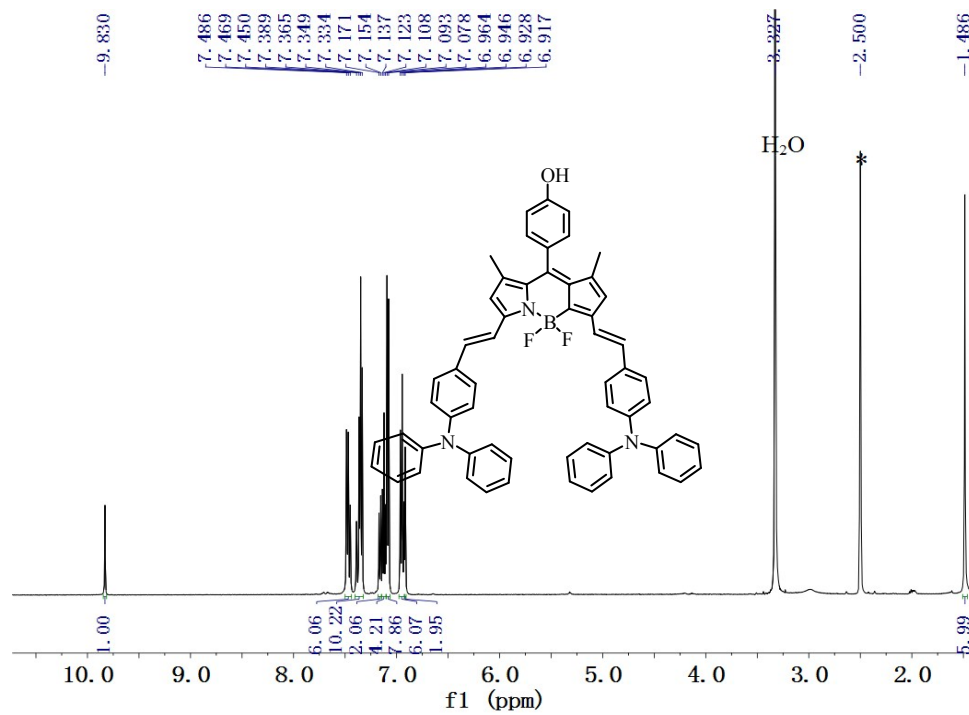


Fig. S6 ¹H NMR spectrum of 3

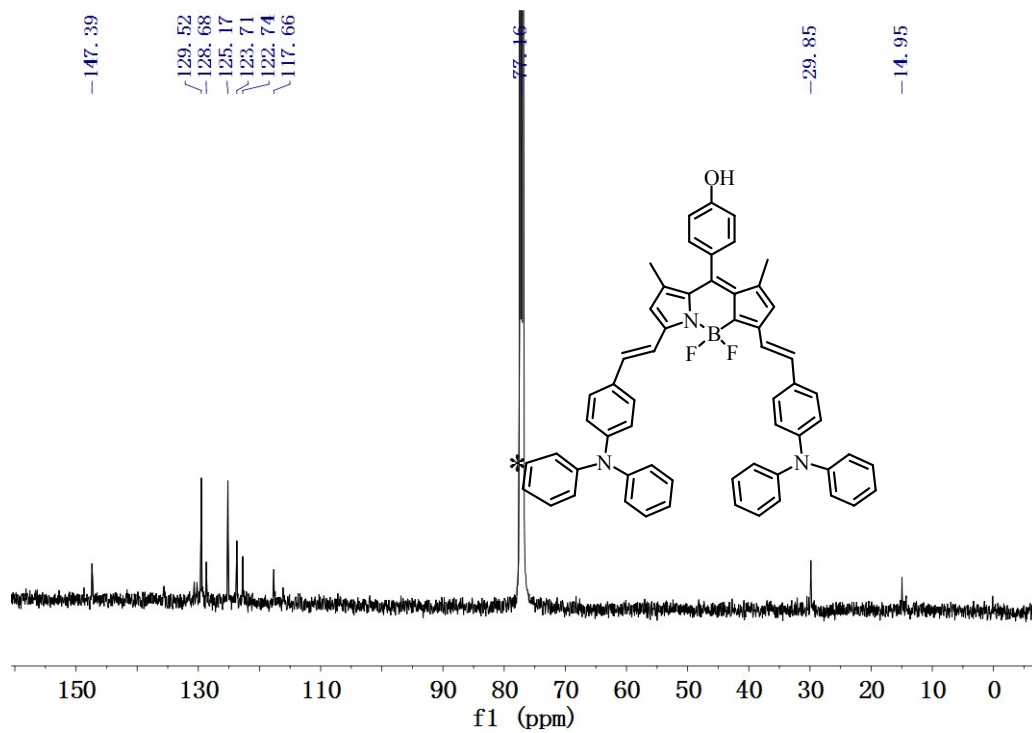


Fig. S7 $^{13}\text{C}\{^1\text{H}\}$ NMR spectrum of **3**

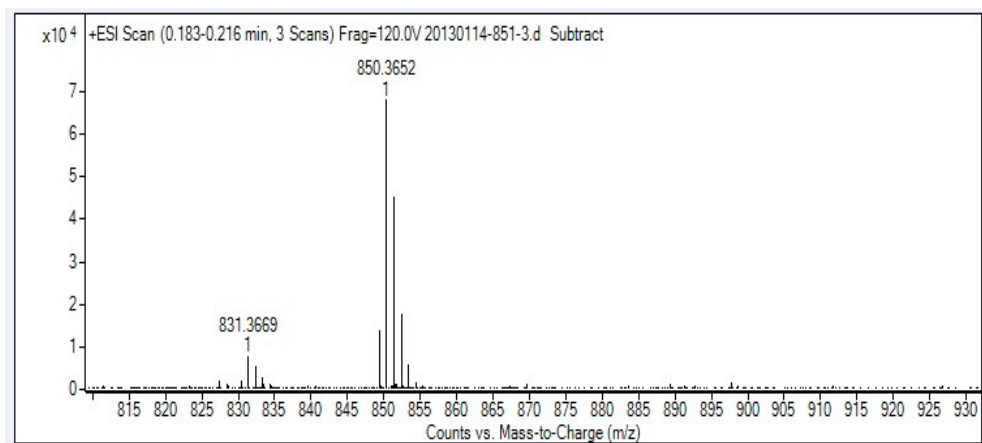


Fig. S8 HRMS spectrum of **3**

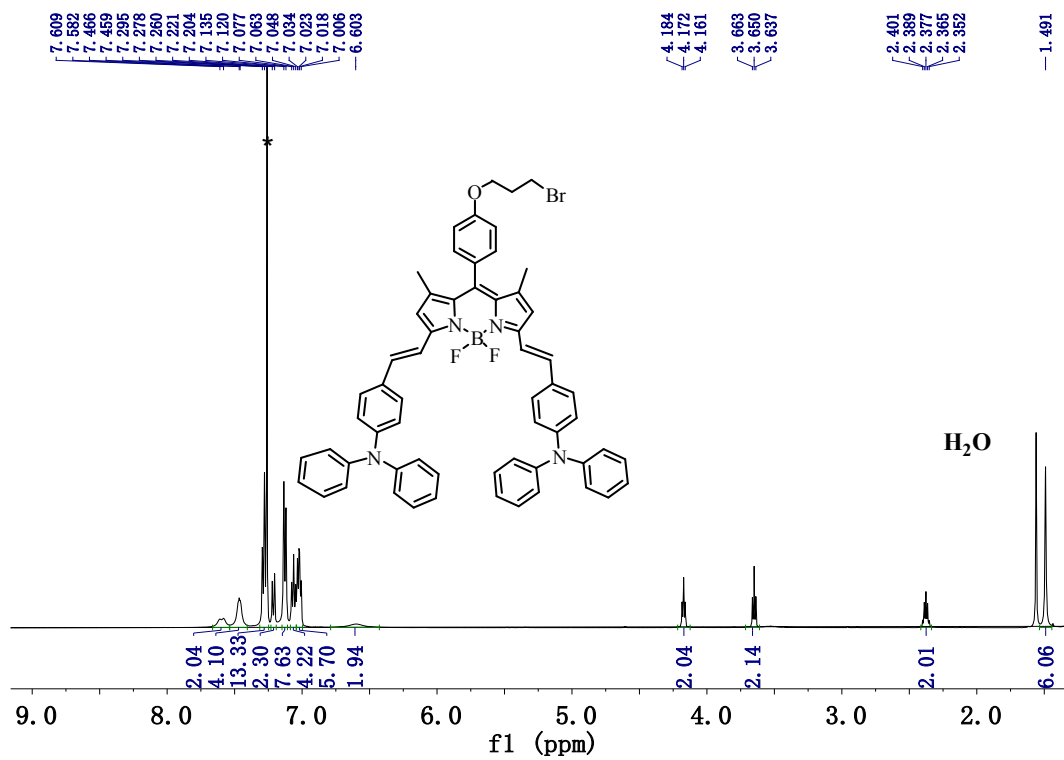


Fig. S9 ¹H NMR spectrum of 4

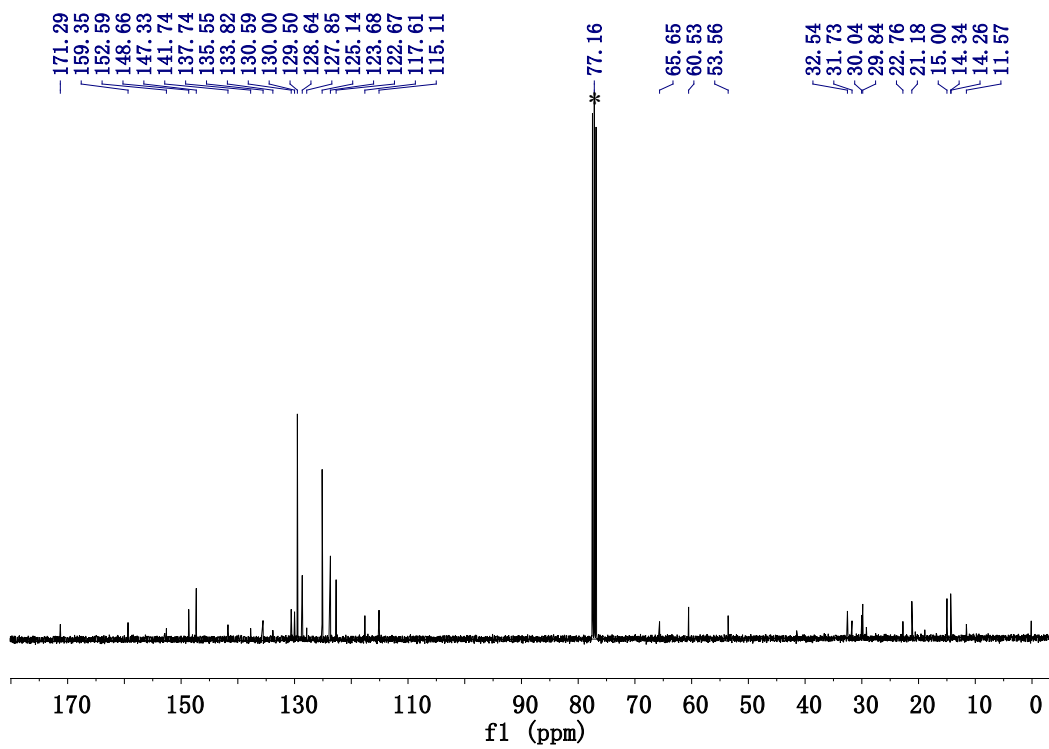


Fig. S10 $^{13}\text{C}\{^1\text{H}\}$ NMR spectrum of **4**

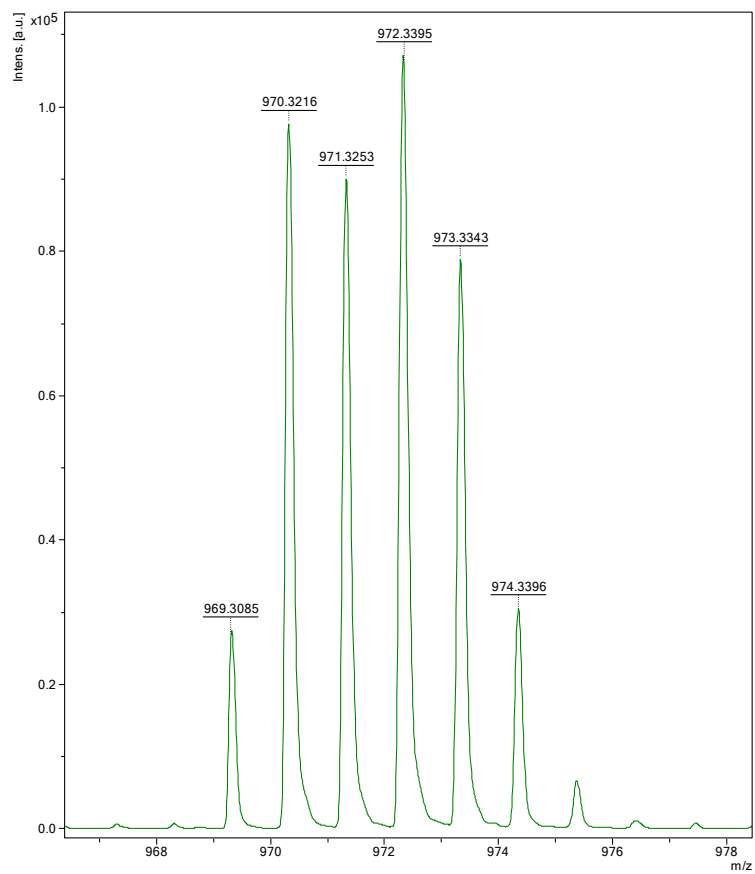


Fig. S11 HRMS spectrum of **4**

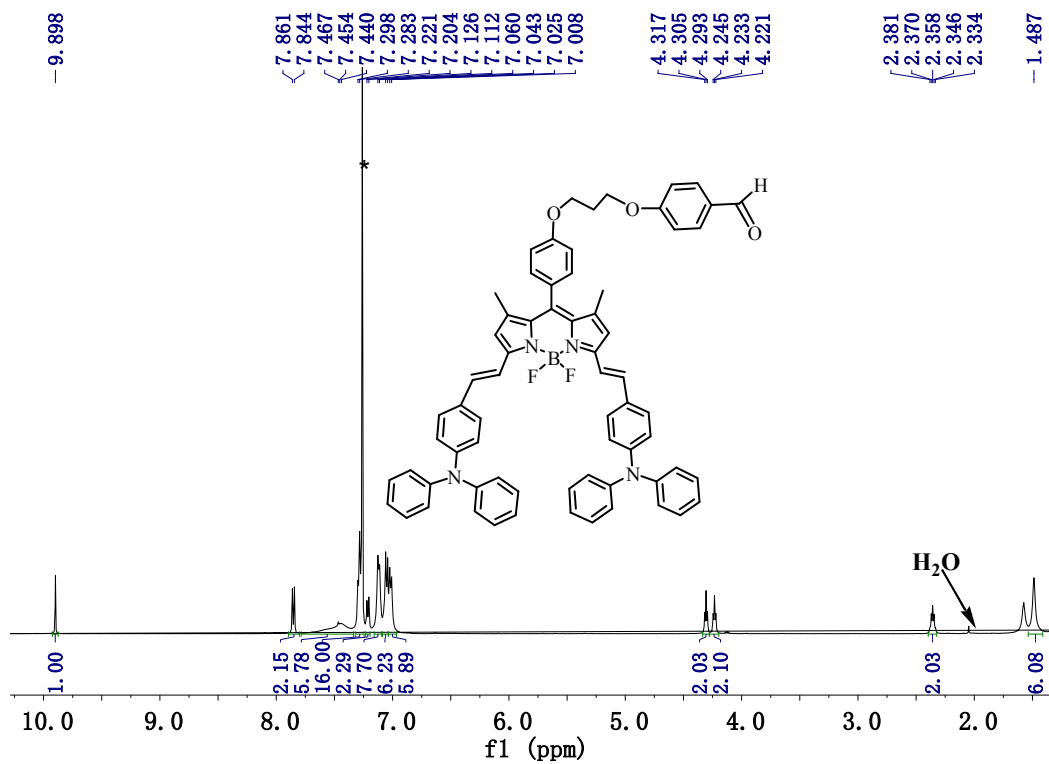


Fig. S12 ¹H NMR spectrum of 5

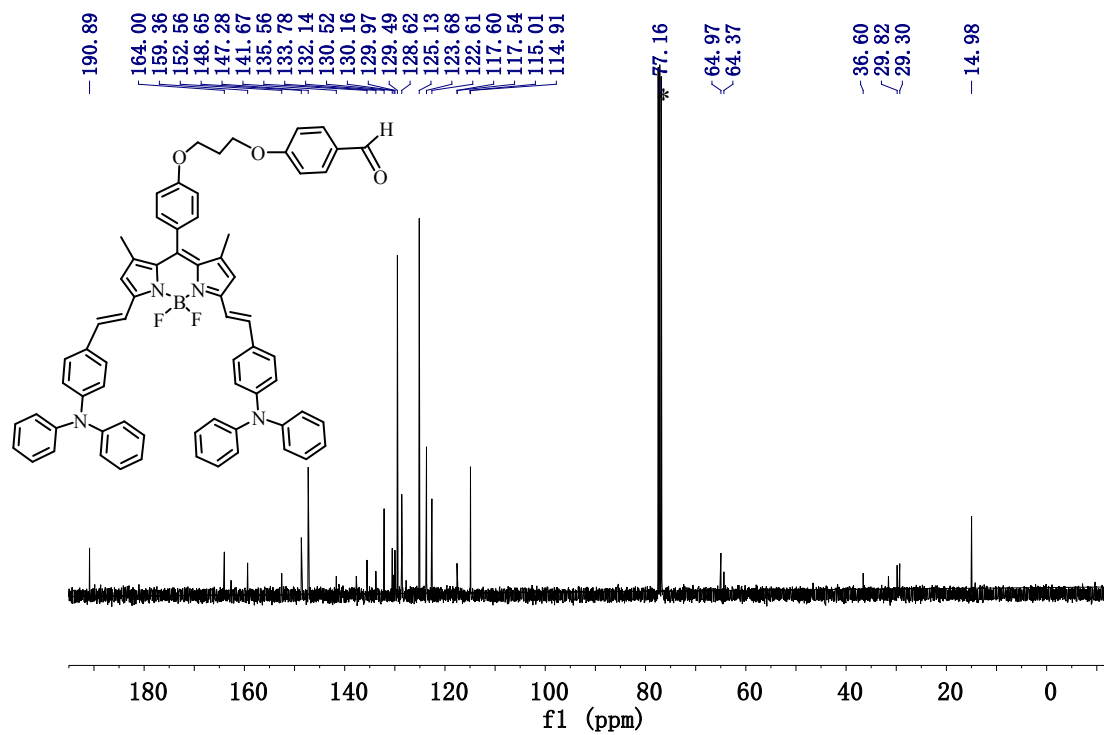


Fig. S13 $^{13}\text{C}\{^1\text{H}\}$ NMR spectrum of **5**

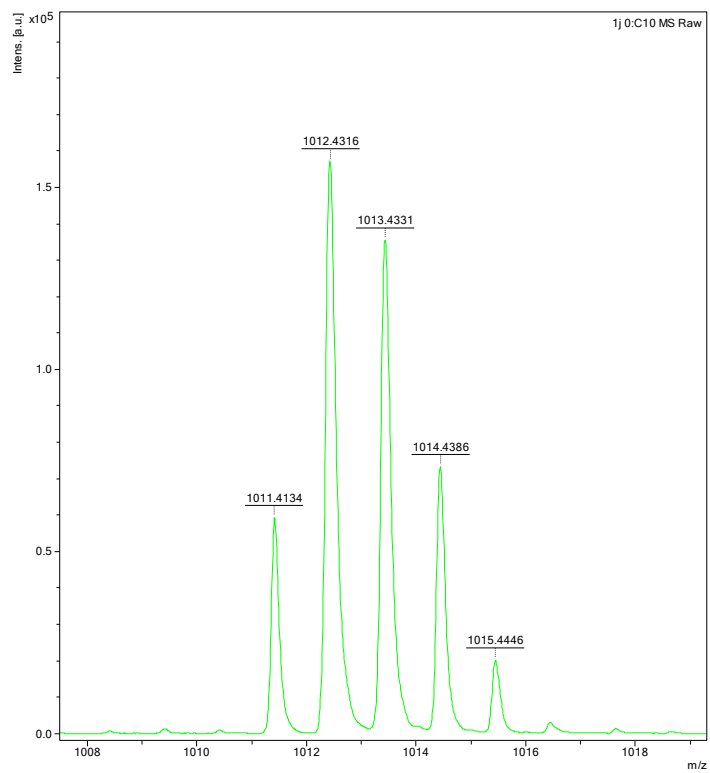


Fig. S14 HRMS spectrum of **5**

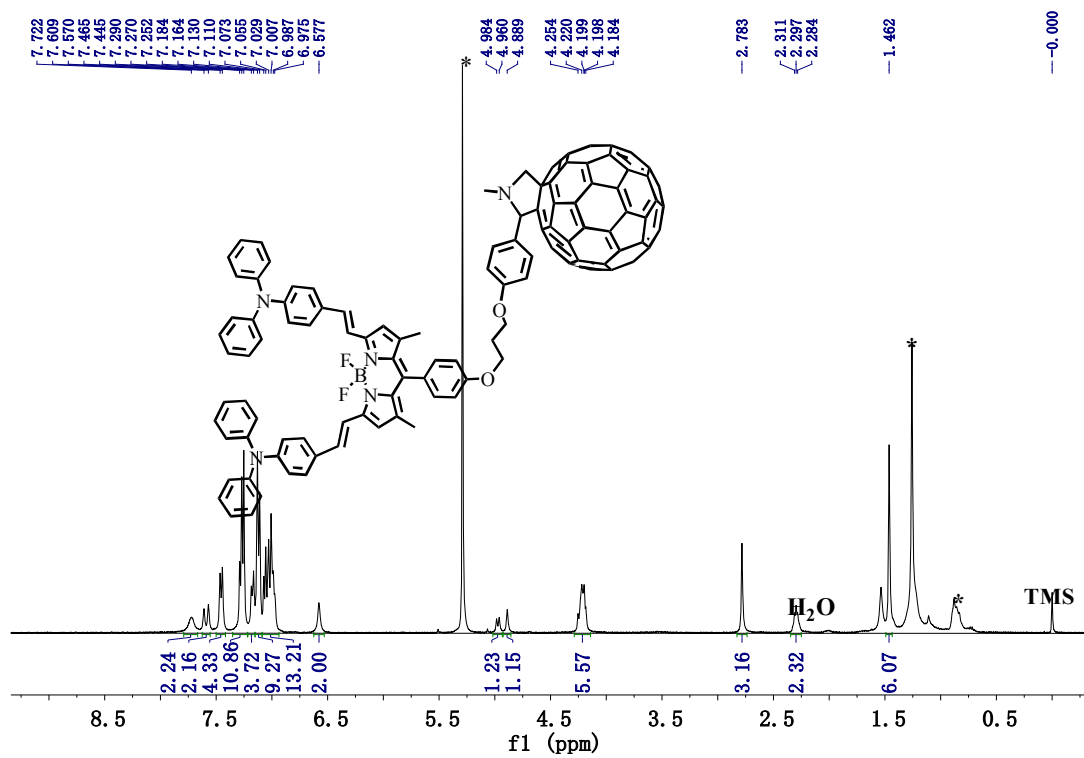


Fig. S15 ¹H NMR spectrum of 6

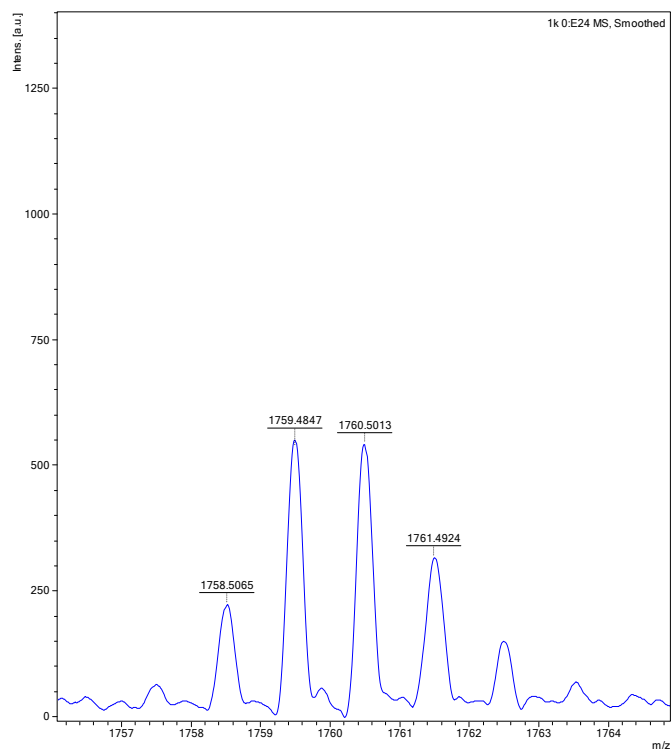


Fig. S16 HRMS spectrum of **6**

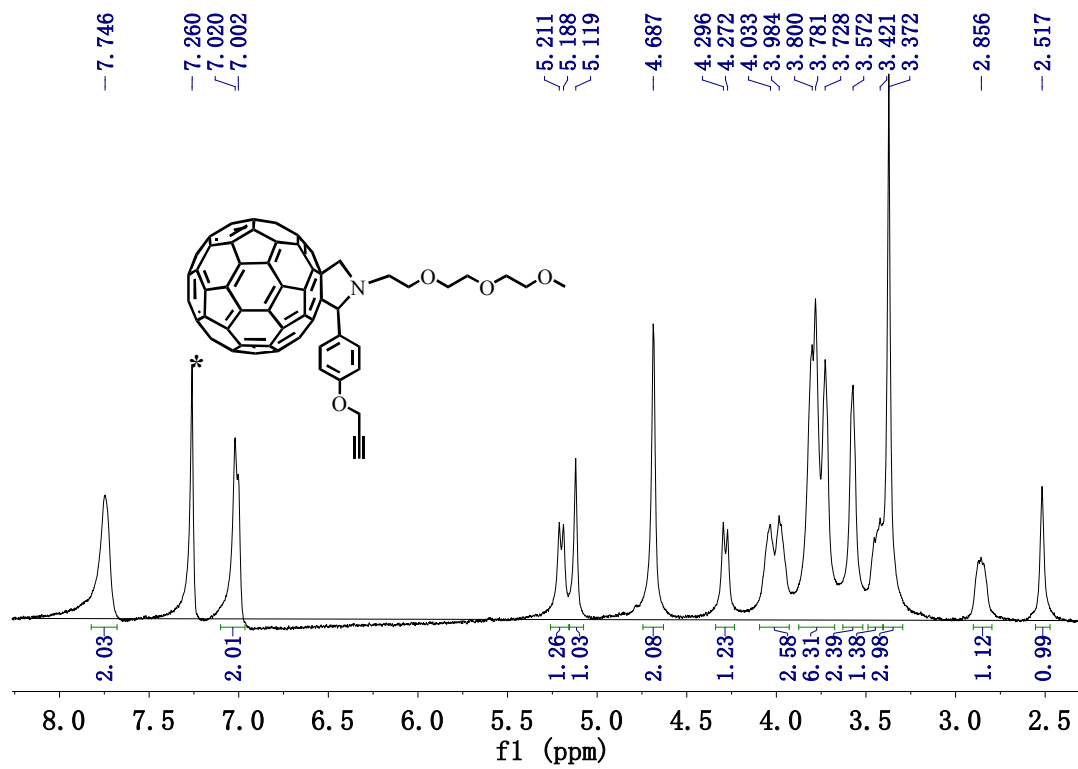


Fig. S17 ¹H NMR spectrum of **9**

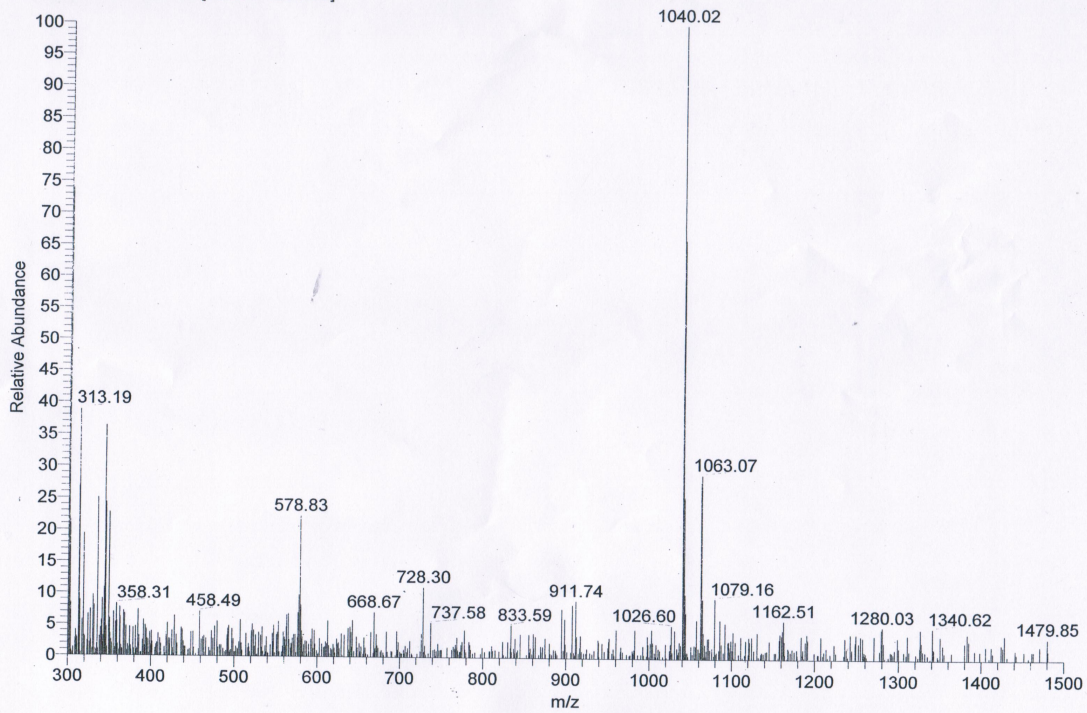


Fig. S18 MS spectrum of **9**